Effects of fines content on the wicking performance of wicking nonwoven geotextiles

Ei Thinzar Moe, Jiming Liu, Minghao Liu & Cheng Lin
Department of Civil Engineering, University of Victoria, Victoria, BC, Canada
Sam Bhat
Titan Environmental Containment Ltd., Ile des Chenes, MB, Canada

ABSTRACT
Seepage of water into road sections increases water content in bases and the subgrade, leading to pavement distresses, such as rutting and cracking. To mitigate this issue, an effective subsurface drainage system is essential, particularly when gravity alone is insufficient to drain the water out. This study explores the use of wicking nonwoven geotextiles (WNWGs) component of a novel Wicking Geotextile-Geogrid composite, as a solution to prevent water accumulation. They, featuring a highly porous microstructure and hydrophilic fibers, can attract and rapidly remove water through their spontaneous and forced wetting and wicking functions. A series of in-soil wicking tests were conducted on saturated sands with different fine contents ranging from 0%, 5%, 10%, to 15% by weight. The water content at four different depths in the soil column was continuously monitored. The findings of this research provide insights into the efficacy of WNWGs in reducing water content in soils with different fines contents and will inform future applications of WNWGs in road construction to improve pavement durability and reduce long-term maintenance requirements.

RÉSUMÉ
L'infiltration d'eau dans les sections routières augmente la teneur en eau dans les couches de base et le sol support, entraînant des détériorations du revêtement, telles que l'orniérage et la fissuration. Pour atténuer ce problème, un système de drainage souterrain efficace est essentiel, particulièrement lorsque la gravité seule est insuffisante pour évacuer l'eau. Cette étude explore l'utilisation de géotextiles non-tissés à effet mèche (WNWGs) comme solution pour prévenir l'accumulation d'eau. Ces géotextiles, caractérisés par une microstructure hautement poreuse et des fibres hydrophiles, peuvent attirer et éliminer rapidement l'eau grâce à leurs fonctions spontanées et forcées de mouillage et d'effet mèche. Une série de tests d'effet mèche en milieu terreux a été réalisée sur des sables saturés avec différentes teneurs en particules fines allant de 0%, 5%, 10%, à 15% en poids. La teneur en eau à quatre profondeurs différentes dans la colonne de sol a été surveillée en continu. Les résultats de cette recherche fournissent des indications sur l'efficacité des WNWGs pour réduire la teneur en eau dans les sols avec différentes teneurs en particules fines et guideront les futures applications des WNWGs dans la construction routière afin d'améliorer la durabilité des chaussées et de réduire les exigences d'entretien à long terme.

1 INTRODUCTION

Water accumulation in base courses and the subgrade is one of the primary causes of pavement distresses such as rutting and potholes. Under heavy traffic loads, excess pore water pressure can develop rapidly in poor drainage conditions, accelerating the degradation of the road structure. Therefore, mitigating the effects of water accumulation is essential for improving the durability and service life of roads. Among various approaches, the use of geosynthetics for subsurface drainage has become a widely adopted and effective strategy in roadway systems.

Nonwoven geotextiles have been employed for drainage applications for more than 50 years (Giroud et al., 2022) and have been the focus of extensive research. Iryo and Rowe (2003) pointed out that nonwoven geotextiles exhibit a steep water retention curve, which means that a small change in suction can cause them to shift from a permeable to an impermeable state. When the hydraulic conductivity of the geotextile drops by several orders of magnitude below that of the surrounding soil, it may begin to reject water flow—an effect referred to as the capillary break effect (Zornberg et al., 2010). As a result, an unsaturated nonwoven geotextile can inadvertently trap water at the soil–geotextile interface, contrary to its intended drainage function.

Conventional nonwoven geotextiles are predominantly made from hydrophobic polymers such as polypropylene and polyester, which repel water. To overcome the limitations imposed by this hydrophobicity, geosynthetics that utilize wicking action have been explored to facilitate water removal from unsaturated soils and bypass the adverse effects of capillary breaks in conventional geotextiles.

To clarify the underlying mechanism, it is important to distinguish between wetting and wicking, as defined in textile science. Wetting refers to the displacement of a fiber-air interface with a fiber-liquid interface, while wicking is the spontaneous flow of a liquid into a porous system driven by capillary forces (Kissa, 1996; Patnaik et al., 2006). Wetting is a prerequisite for wicking, as capillary action requires a liquid to wet the fibers assembled within capillary spaces. Hence, conventional nonwoven geotextiles made of hydrophobic fibers generally lack the ability to exhibit true wicking behavior.

Stormont et al. (2001) demonstrated that geocomposites incorporating fiberglass woven geotextiles—due to fiberglass's high water affinity—could effectively wick moisture from unsaturated soils. Later, wicking woven geotextiles have been introduced (Zhang et al., 2014; Guo et al., 2017, 2021; Zaman et al., 2022, 2024). These geotextiles consist of woven fabrics embedded with hydrophilic and hygroscopic nylon filaments with multichannel cross-sections, which generate strong capillary suction for moisture removal. Multiple laboratory and field studies have confirmed the ability of these geotextiles to remove moisture under both saturated and unsaturated conditions. More recently, a wicking nonwoven geotextile (WNWG) has been introduced. It retains the high porosity of nonwoven structures while incorporating hydrophilic fibers to promote wetting and wicking. The high wettability and efficient moisture removal properties of WNWGs have been validated in recent studies (Jarjour et al., 2024; Liu et al., 2024; Liu et al., 2025). However, these studies did not thoroughly examine the wicking performance of WNWGs considering the influence of soil fine content on their effectiveness. To address this gap, the present study investigates the performance of WNWG in soils with varying fine contents. A series of laboratory-scale tests were conducted to characterize the drainage behavior of soils in the presence of WNWG.

2 METHODS AND MATERIALS

2.1 Materials and Equipment

To evaluate in-soil wicking performance of the WNWG, an experiment was designed where the WNWG served as the only drainage path within a soil column. The test setup is illustrated in Figure 1. A strip of WNWG was sandwiched between two soil columns housed in standard steel compaction molds. To ensure that drainage occurred only through the WNWG, all other potential drainage paths—namely the top and bottom of the specimen—were sealed with plastic sheets or wraps. Volumetric moisture content (VMC) sensors were installed at multiple depths to capture changes in moisture and assess the drainage behavior of WNWG in soils.

Material properties of WNWG are shown in Table 1. The WNWG is a component of a novel wicking geotextile-geogrid composite, supplied by Titan Environmental Containment Ltd. This study focusses on the performance of the wicking geotextile; therefore, the geogrid component was not included in the tests. Photos of the composite and the WNWG are shown in Figure 2.

Four soil specimens with different fine contents were used in this test. Sand and kaolin were mixed in different dry weight ratios to create soils with different fine contents: 100:0, 95:5, 90:10, and 85:15(sand: kaolin). These specimens were labeled K0S100, K5S95, K10S90, and K15S85, respectively. For instance, K5S95 denotes a specimen consisting of 5% kaolin and 95% sand by dry weight.

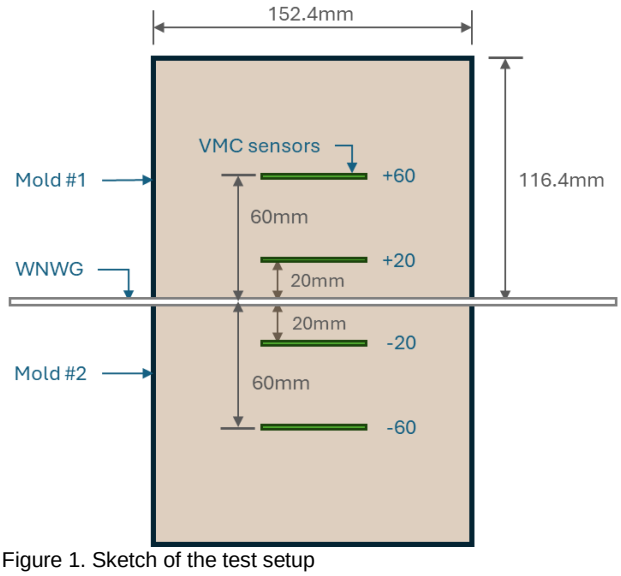

Figure 1. Sketch of the test setup

Table 1. Material properties of WNWG*

Properties	WNWG	Test Method
Apparent opening size, AOS (μm)	194	ASTM D4751
Mass per unit area, M_A (g/m^2)	247	ASTM D5261
Fiber radius, r_f (μm)**	8.8	-
Permittivity (sec^{-1})	1.82	ASTM D4491
Flow rate (L/min/m^2)	5543	ASTM D4491
Grab strength (N)	962	ASTM D4632
Trapezoidal tear (N)	396	ASTM D4533
CBR puncture strength (N)	2830	ASTM D6241

*Data provided by Titan and tested by SGI Testing Services, LLC in 2022.
** Measured from Scanning Electron Microscopy (SEM) analysis.

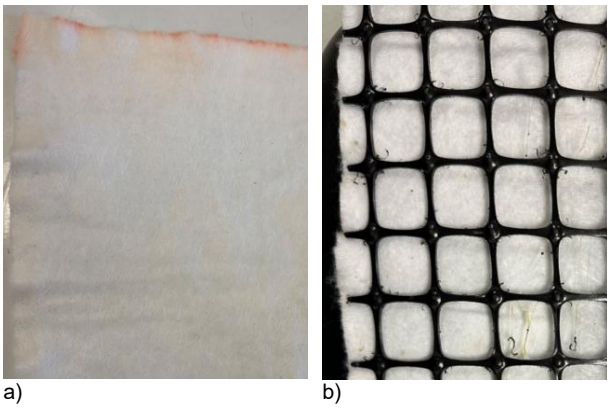
a) b)
Figure 2. Photos of geosynthetics: a) WNWG and b) wicking geotextile-geogrid composite

The sand used in the experiment was acquired from a local quarry yard in Victoria, BC, Canada, and classified as poorly graded sand (SP), with a mean particle size (D_{50}) of 0.72 mm and a specific gravity of 2.7. It has a maximum dry density of 1.90 g/cm^3 and an optimum water content of

10.1%, as determined by the standard proctor compaction tests (ASTM D698-12). The kaolin used in this experiment was a commercial EPK kaolin sourced from Edgar Minerals.

In each test, a 160 mm x 480 mm section of WNWG was sandwiched between the two molds. Inside the container, the geotextile was in direct contact with the soil, allowing it to wick or drain water, while the exposed portion of the geotextile outside the container remained in contact with the air.

Two six-inch standard Proctor compaction molds (ASTM D698-12, 2021) were used as soil containers, each with an inner diameter of 152.4 mm and a height of 116.4 mm. Four EC-5 VMC sensors (METER Group) were embedded at vertical distances of 20 mm and 60 mm above and below the WNWG. Designating the WNWG position as 0 mm, the four sensor locations were: +60 mm, +20 mm, –20 mm, and –60 mm, as shown in Figure 1. These labels are also used in the results section for clarity. A CR1000X data logger (Campbell Scientific) was used for data acquisition, with VMC recorded at one-minute intervals.

2.2 Specimen Preparation

Each soil type was conditioned to its optimum moisture content and compacted to 95% of its maximum dry density and then was further saturated by adding water to it. Standard proctor tests were conducted for each soil type to establish compaction curves and determine target densities for specimen compaction (Table 2) and moisture contents under saturated conditions. The amount of additional water required to fill the specimen's voids after compaction was calculated accordingly.

Table 2. Compaction test results of soils

Specimen	Optimum moisture content (%), gravimetric	Maximum dry density (g/cm^3)
K0S100	10.1	1.90
K5S95	8.3	1.93
K10S90	9.2	2.10
K15S95	9.8	2.12

For every specimen, two compacted soil columns were prepared using the six-inch molds. The procedure for specimen assembly is outlined below:
(1) Line the interior of the bottom mold with plastic sheets.
(2) Compact the bottom soil column in three lifts and install two VMC sensors at the designated depths.
(3) Pour a calculated volume of water into the bottom mold to initiate saturation (Figure 3a).
(4) Place the WNWG on top of the bottom mold, covering it with plastic sheets to prevent premature wetting or wicking (Figure 3b).
(5) Repeat steps 2 and 3 for the top soil column (Figure 3c).
(6) Start the test by removing the plastic sheets from the WNWG and begin VMC monitoring (Figure 3d), continuing until reading stabilizes.

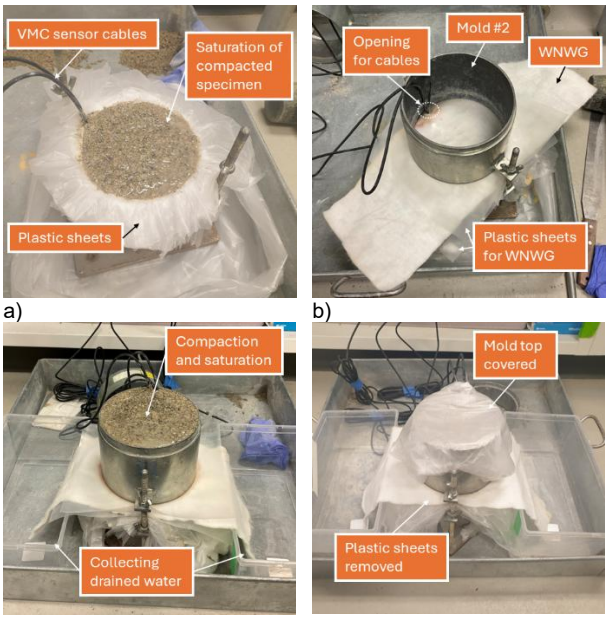

Figure 3. Specimen installation procedures

To minimize evaporation and eliminate leakage, a few layers of plastic sheets were used to line the bottom mold, block water from WNWG before tests initiate, and cover the top surface of soils in the top mold.

The quantity of water added after compaction for each specimen is summarized in Table 3. Since full saturation through infiltration alone is difficult to achieve, the bottom mold was allowed to absorb water as much as possible for one hour before continuing with the upper column. The top mold was given sufficient time to absorb its designated amount of water before the start of the test. Accordingly, the "Total" row under "Top Mold" in Table 3 reflects the volume of water used to saturate each mold. The protective plastic sheets around the WNWG were only removed once saturation was deemed complete. For the K15S85 specimen, additional small volumes of water were added after each lift to expedite saturation due to its lower permeability.

Table 3. Amount of excess water added to the specimens

Mold	Lift	Excess water added (g)			
		K0S100	K5S95	K10S90	K15S85
Top Mold	Lift 3	312	261	166.7	105.6
	Lift 2	0	0	0	4.0
	Lift 1	0	0	0	4.4
	Total	312	261	166.7	114.0
Bottom Mold	Lift 3	246	161	32.2	34.4
	Lift 2	0	0	0	10.7
	Lift 1	0	0	0	9.0
	Total	246	161	32.2	54.1

3 RESULTS

3.1 Time History of VMC

Figures 4 to 7 illustrate the changes in volumetric moisture content (VMC) over time for each specimen. Significant water removal was observed in all specimens except K15S85, where the VMC change remained within 1% throughout the test.

For the K0S100 specimen (Figure 4), rapid drainage occurred in the top mold, with both upper sensors registering an almost immediate reduction in VMC. In the bottom mold, the VMC exhibited a sharp decline around 15 hours into the test following a short plateau at the –20 mm location. A similar trend was observed at –60 mm, although the drop occurred later, around 133 hours after the start.

The K5S95 specimen (Figure 5) showed a similar drainage pattern to K0S100 but at a slower rate. An immediate VMC drop was observed at +60 mm, consistent with K0S100. At +20 mm, a rapid decrease began approximately 42 hours into the test. Interestingly, VMC values at –20 mm and –60 mm slightly increased during the initial phase, likely due to infiltration through the WNWG. After 100 hours, both locations began to exhibit steady declines, marking the start of draining at these depths.

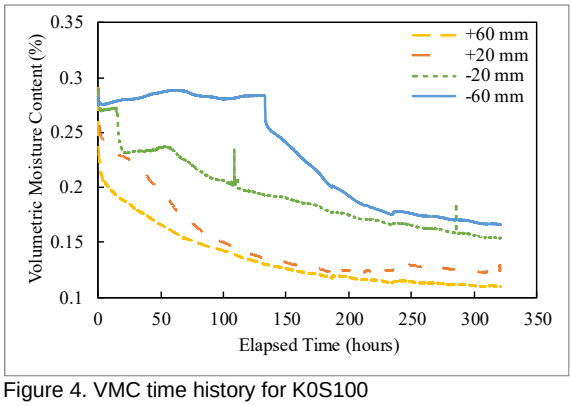

Figure 4. VMC time history for K0S100

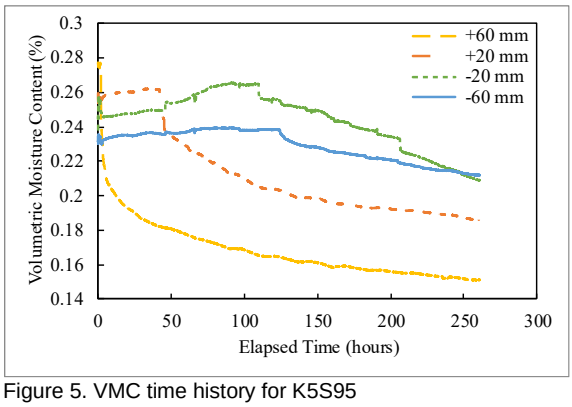

Figure 5. VMC time history for K5S95

In the K10S90 specimen (Figure 6), VMC reductions at each depth were further delayed. The +60 mm sensor showed a pronounced drop around 150 hours, whereas the same location responded immediately in K0S100 and K5S95. Accelerated VMC reductions were observed at +20 mm and –20 mm after approximately 260 hours. At –60 mm, the VMC only decreased by 1.1% of its initial VMC over the entire test, indicating minimal influence from the WNWG at that depth.

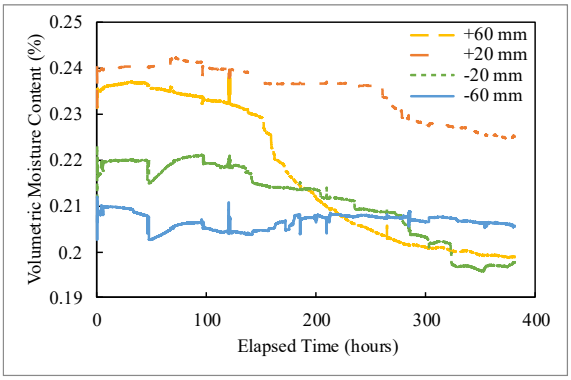

Figure 6. VMC time history for K10S90

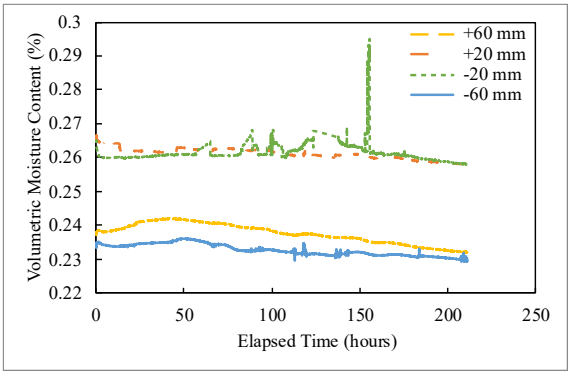

Figure 7. VMC time history for K15S85

Across K0S100, K5S95, and K10S90 specimens, a clear sequence in moisture reduction emerged—from +60 mm to +20 mm, then to –20 mm and –60 mm. This sequence can be explained by changes in pore pressure. At +20 mm, for example, water loss was initially offset by replenishment from above, leading to a steady VMC phase. As the water head continued to decline, pore pressure at that depth decreased, reducing the water supply and eventually triggering rapid drainage. This delayed response is reflected in the VMC drops shown in Figures 4 and 5. For depths below the WNWG, the rapid VMC drops were most likely the result of wicking-driven drainage, since all other drainage paths were sealed with multiple plastic layers. No signs of leakage were observed at the bottom of the specimens during disassembly.

To further validate the drainage effect, gravimetric moisture content (GMC) measurements were taken at multiple depths in the K0S100 specimen after testing. Results are shown in Table 4. Soil samples were collected within approximately 10 mm above and below each target depth. The +90 mm and –90 mm locations correspond to the upper and lower ends of the specimen, respectively, given the mold height of 110.6 mm.

Table 4. Final gravimetric moisture contents in K0S100

Location	+90	+60	+20
GMC (%)	4.7	4.7	5.4
Location	-20	-60	-90
GMC (%)	6.5	6.9	10.0

GMC values at all depths were significantly lower than the initial values following specimen preparation. Theoretical initial GMCs for the top and bottom molds were estimated at 18.2% and 16.5%, respectively, based on water added (Table 3). The final GMC of 10.0% at –90 mm confirms that water in the lower portion of the specimen was actively removed and that the WNWG's influence extended beyond 90 mm below its interface.

3.2 VMC Profile and Effectiveness of Wicking

Figures 8 to 11 present VMC profiles at selected timestamps: the start of the test, 24 hours, 48 hours, 96 hours, and the end of the test (specific end times vary for each specimen). These profiles illustrate the spatial progression of moisture changes over time.

The K0S100 specimen (Figure 8) showed progressive drainage above –60 mm during the first 96 hours, likely due to a combined effect of gravity and capillary suction from the WNWG. Between 96 hours and the end of the test, the majority of moisture reduction occurred below the WNWG, especially at -60mm, where VMC dropped from 28.1% to 16.6%, indicating that wicking action was able to draw water upward from the lower column against gravity, aided by soil capillarity.

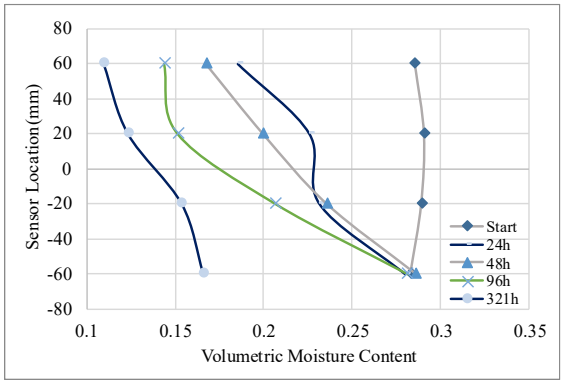

Figure 8 VMC profiles for K0S100 specimen

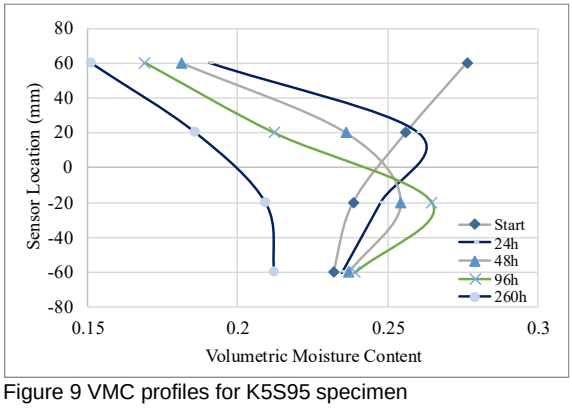

Figure 9 VMC profiles for K5S95 specimen

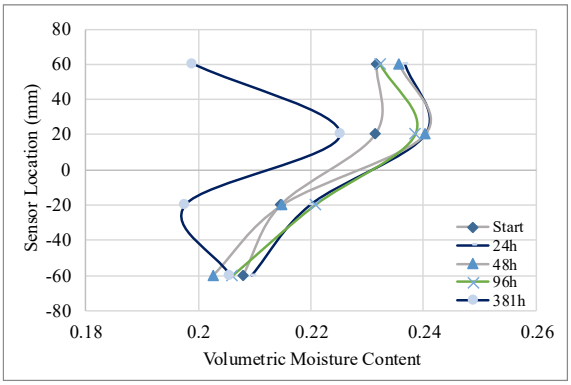

Figure 10 VMC profiles for K10S90 specimen

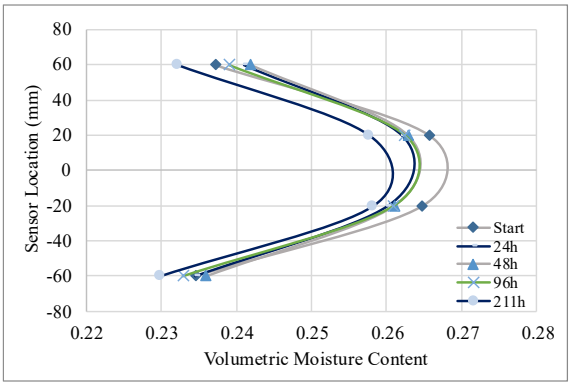

Figure 11 VMC profiles for K15S85 specimen

The K5S95 specimen (Figure 9) showed a distinct infiltration pattern. VMC profiles at 24, 48, and 96 hours revealed a migrating peak moving downward from +20 mm to –20 mm. The VMC at these peaks exceeded the initial VMC values, suggesting that a small amount of water may have infiltrated through the WNWG. However, this infiltration was minor compared to the amount of water drained through the in-plane path of the WNWG.

For the K10S90 specimen (Figure 10), water infiltration was slow, and only limited VMC reductions were observed at +60 mm, +20 mm, and –20 mm by the end of the test. Notably, the –20 mm depth experienced more drying than +20 mm, likely due to reduced water replenishment from above and enhanced capillary suction in finer soils. The K15S85 specimen (Figure 11) showed negligible VMC change throughout the test, indicating that soils with high fine content severely limit the effectiveness of the WNWG.

Table 5 summarizes the reduction in VMC for each specimen from the start to the end of the tests. As the fine content in the soil increased, the rate and extent of drainage progressively decreased. Nevertheless, the influence of the WNWG remained evident, particularly in specimens with up to 10% fines. While the drainage rate was lower and the zone of influence narrower in these cases, the WNWG still contributed to measurable moisture reduction. In contrast, soils with a high fine content—such as the 15% kaolin mixture—proved too impermeable for effective wicking. Based on these findings, the use of WNWGs is recommended primarily for soils with low fine content.

Table 5 VMC reduction (%) for each specimen

Location	VMC reduced (%)			
	K0S100	K5S95	K10S90	K15S85
+60mm	-17.6	-12.5	-3.3	-0.5
+20mm	-16.7	-7.0	-0.6	-0.8
-20mm	-13.5	-2.9	-1.7	-0.7
-60mm	-11.7	-2.0	-0.2	-0.4

4 CONCLUSIONS

This study presented a straightforward laboratory method to evaluate the in-soil performance of a wicking nonwoven geotextile (WNWG) across soils with varying fine contents. Two standard compaction molds were used to create a vertically aligned soil column, with the WNWG placed at the interface to serve as the sole drainage path. Nearly saturated specimens were prepared to the best extent possible, and volumetric moisture content (VMC) was monitored at multiple depths over a period of eight to sixteen days, until readings stabilized.

Based on the results of this study, the following conclusions could be drawn:

- The WNWG effectively removed moisture from nearly all depths in the clean sand specimen (K0S100).
- Moisture reduction was observed in soils with fine content up to 10%, with the most pronounced wicking effect occurring in soil with less than 5% fines, both in terms of rate and volume of drainage.
- The vertical influence of the WNWG extended throughout the entire soil column in low-fines specimens but diminished to approximately 20 mm below the interface in soils with 10% fines.
- No signs of moisture accumulation or capillary break were observed near the WNWG in any of the tests.

These findings highlight the potential of WNWGs as a drainage enhancement solution in pavement applications, particularly in coarse-grained or low-fines soils. The observed wicking behavior confirms that WNWGs can operate effectively without exhibiting capillary break, supporting their reliability in unsaturated conditions. However, their drainage efficiency becomes severely limited in soils with high fine content (e.g., 15% kaolin), suggesting a performance threshold tied to soil permeability.

Further research is recommended to quantitatively assess the benefits of WNWGs in soil through controlled comparisons with conventional nonwoven geotextiles, and to incorporate pore water pressure or matric suction measurements to better understand the capillary mechanisms driving drainage within and beneath the WNWG.

5. ACKNOWLEDGMENTS

The authors thank NSERC/ MITACS and University of Victoria for the financial support as well as the industrial partner, Titan Environmental Containment Ltd., for supplying the product and providing technical and financial support.

REFERENCE

Giroud, J. P., Han, J., Tutumluer, E., & Dobie, M. J. D. (2022). The use of geosynthetics in roads. *Geosynthetics International*, 1–34.

Guo, J., Wang, F., Zhang, X., & Han, J. (2017). Quantifying Water *Removal* Rate of a Wicking Geotextile under Controlled Temperature and Relative Humidity. *Journal of Materials in Civil Engineering*, *29*(1), 04016181.

Guo, J., Han, J., Zhang, X., & Li, Z. (2021). Experimental evaluation of wicking geotextile-stabilized aggregate bases over subgrade under rainfall simulation and cyclic loading. *Geotextiles and Geomembranes*, *49*(6), 1550–1564.

Iryo, T., & Rowe, R. K. (2003). On the hydraulic behavior of *unsaturated* nonwoven geotextiles. *Geotextiles and Geomembranes*, *21*(6), 381–404.

Jarjour, J., Meguid, M., & Bhat, S. (2024). Water retention *characterization* of non-woven geotextiles: An application for wicking materials. *E3S Web of Conferences*, *569*, 12003.

Kissa, E. (1996). Wetting and Wicking. *Textile Research* Journal, *66*(10), 660–668.

Liu, J., Lin, C., Liu, M., & Bhat, S. (2024). Repeated load triaxial tests of WickGrid stabilized base materials. *E3S Web of Conferences*, *569*, 21006.

Liu, M., Liu, J., Bhat, S., Gao, Y., & Lin, C. (2025). Model tests on wicking geosynthetic composite *reinforced* bases over weak subgrade. *Geotextiles and Geomembranes*, *53*(4), 938–949.

Patnaik, A., Rengasamy, R. S., Kothari, V. K., & Ghosh, A. (2006). *Wetting* and Wicking in Fibrous Materials. *Textile Progress*, *38*(1), 1–105.

Stormont, J. C., Ramos, R., & Henry, K. S. (2001). Geocomposite Capillary Barrier Drain System with *Fiberglass* Transport Layer. *Transportation Research Record: Journal of the Transportation Research Board*, *1772*(1), 131–136.

Zaman, Md. W., Han, J., & Zhang, X. (2022). Technical Review of *Development* and Applications from Wicking Fabric to Wicking Geotextile. *Geo-Congress 2022*, 587–596.

Zaman, M. W., Han, J., Kabir, M. U., & Parsons, R. L. (2024). Laboratory evaluation of wicking geotextile for moisture reduction in silty sands at different fines contents. *Geotextiles and Geomembranes*, *52*(6), 1180–1190.

Zhang, X., Presler, W., Li, L., Jones, D., & Odgers, B. (2014). Use of Wicking Fabric to Help Prevent Frost Boils in Alaskan Pavements. *Journal of Materials in Civil Engineering*, *26*(4), 728–740.

Zornberg, J. G., Bouazza, A., & McCartney, J. S. (2010). Geosynthetic capillary barriers: Current state of knowledge. *Geosynthetics International*, *17*(5), 273–300.